HHS Public Access

Author manuscript

J Alzheimers Dis. Author manuscript; available in PMC 2018 October 05.

Published in final edited form as:

J Alzheimers Dis. 2017 ; 60(Suppl 1): S133–S150. doi:10.3233/JAD-170342.

Chromatin-Bound Oxidized α-Synuclein Causes Strand Breaks in Neuronal Genomes in *in vitro* Models of Parkinson's Disease

Velmarini Vasquez[a,b,c], **Joy Mitra**[a], **Pavana M. Hegde**[a], **Arvind Pandey**[a], **Shiladitya Sengupta**[a,e], **Sankar Mitra**[a,e], **K. S. Rao**[b,*], and **Muralidhar L. Hegde**[a,d,e,*]

[a]Department of Radiation Oncology, Houston Methodist Research Institute, Houston, TX, USA

[b]Centre for Neuroscience, Instituto de Investigaciones Científicas y Servicios de Alta Tecnología, City of Knowledge, Republic of Panama

[c]Department of Biotechnology, Acharya Nagarjuna University, Guntur, India

[d]Houston Methodist Neurological Institute, Institute of Academic Medicine, Houston Methodist Hospital, Houston, TX, USA

[e]Weill Cornell Medical College of Cornell University, NY, USA

Abstract

Alpha-synuclein (α-Syn) overexpression and misfolding/aggregation in degenerating dopaminergic neurons have long been implicated in Parkinson's disease (PD). The neurotoxicity of α-Syn is enhanced by iron (Fe) and other pro-oxidant metals, leading to generation of reactive oxygen species in PD brain. Although α-Syn is predominantly localized in presynaptic nerve terminals, a small fraction exists in neuronal nuclei. However, the functional and/or pathological role of nuclear α-Syn is unclear. Following up on our earlier report that α-Syn directly binds DNA *in vitro*, here we confirm the nuclear localization and chromatin association of α-Syn in neurons using proximity ligation and chromatin immunoprecipitation analysis. Moderate (~2-fold) increase in α-Syn expression in neural lineage progenitor cells (NPC) derived from induced pluripotent human stem cells (iPSCs) or differentiated SHSY-5Y cells caused DNA strand breaks in the nuclear genome, which was further enhanced synergistically by Fe salts. Furthermore, α-Syn required nuclear localization for inducing genome damage as revealed by the effect of nucleus versus cytosol-specific mutants. Enhanced DNA damage by oxidized and misfolded/oligomeric α-Syn suggests that DNA nicking activity is mediated by the chemical nuclease activity of an oxidized peptide segment in the misfolded α-Syn. Consistent with this finding, a marked increase in Fe-dependent DNA breaks was observed in NPCs from a PD patient-derived iPSC line harboring triplication of the *SNCA* gene. Finally, α-Syn combined with Fe significantly promoted neuronal cell death. Together, these findings provide a novel molecular insight into the direct role

*Correspondence to: Muralidhar L. Hegde, PhD, Department of Radiation Oncology, Houston Methodist Research Institute, Fannin St., Smith 8-05, Houston, Texas 77030, USA. Tel.: +1 713 441 7456; Fax: +1 713 790 3755; mlhegde@houstonmethodist.org. and K.S. Rao, Centre for Neuroscience, Instituto de Investigaciones Científicas y Servicios de Alta Tecnología (INDICASAT AIP), City of Knowledge, Republic of Panama. kjr5n2009@gmail.com.

SUPPLEMENTARY MATERIAL

The supplementary material is available in the electronic version of this article: http://dx.doi.org/10.3233/JAD-170342.

of α-Syn in inducing neuronal genome damage, which could possibly contribute to neurodegeneration in PD.

Keywords

Alpha-synuclein; iPSC-derived neural progenitor cells; iron; neurodegeneration; Parkinson's disease

INTRODUCTION

Alpha-synuclein (α-Syn) is a 140 amino acid-containing, intrinsically disordered protein found to be differentially expressed with age and subtypes of neurons in vertebrates [1, 2]. Missense mutations and triplication of α-Syn encoding *SNCA* gene have been linked to neurodegeneration in Parkinson's disease (PD) and related disorders [3–5]. The factors triggering α-Syn mediated neurotoxicity in sporadic PD cases are still vague; however, multiple lines of evidence link pro-oxidant metal dyshomeostasis in affected brain regions and oxidative stress to α-Syn aggregation [6–8]. The interaction of α-Syn with iron (Fe) or copper (Cu) not only affects its folding properties but also its interaction with other macromolecules, including membrane lipids, and cellular localization [9–11]. Furthermore, α-Syn has been shown to oxidize both *in vitro* and *in cell* under PD conditions [12, 13]. While the biological implications of these modifications have not been investigated, oxidation seems to promote α-Syn misfolding *in vitro* [14, 15].

α-Syn is localized predominantly in the neuronal cytosol and is membrane-bound in presynaptic nerve terminals, although several studies identified a small fraction of the protein in other cellular compartments, including the mitochondria and the nucleus [16–22]. Although there are discrepancies in the literature about the presence of α-Syn in the nuclei of healthy neurons, presumably due to varying sensitivity of the detection methods employed, there is more consistent evidence supporting its nuclear localization in PD-affected neurons [23–25]. While the relative abundance of α-Syn in the nucleus versus cytoplasm in various cell types has not been thoroughly investigated, it appears that about 5–10% of α-Syn localizes to the nucleus in cultured neurons. Nonetheless, the precise role of nuclear α-Syn in normal or PD-affected neurons is not known. We previously showed that recombinant α-Syn binds naked DNA *in vitro*, resulting in conformational changes in DNA and protein [26, 27]. Subsequent studies from other laboratories not only confirm this observation but also demonstrate its association with histone H3 in neuroblastoma cells, suggesting its possible role in chromatin [23]. Interestingly, a recent study shows that α-Syn selectively binds to promoter regions of several genes in oxidatively stressed cells, suggesting its involvement in transcriptional regulation [21]. We previously showed affinity of α-Syn for guaninecytosine-rich DNA sequences, a scenario consistent with its proposed promoter activity [28].

One major feature of PD pathology is the accumulation of various types of genome damage in affected neurons [29]. Interestingly, the level of DNA damage accumulation in PD-affected brain regions seems to broadly correlate with disease severity, which is linked to α-Syn pathology and metal accumulation/oxidative stress [29–31]. However, a direct link

between α-Syn toxicity and genome damage has not been investigated. Here, we tested the hypothesis that nuclear α-Syn together with transition metals contribute to neuronal genome damage in PD. Using multiple *in vitro* neuronal models, including neurons from normal and PD patient-derived induced pluripotent stem cells (iPSCs) and α-Syn inducible neuroblastoma line, we demonstrate here for the first time that α-Syn not only associates with chromatin but it also induces DNA breaks in chromatin upon oxidation, leading to neuronal apoptosis. Furthermore, the DNA damage accumulation is dependent on chromatin-bound α-Syn in the neuronal nuclei, consistent with its DNA nicking activity *in vitro*, both of which are facilitated by pro-oxidant Fe and α-Syn misfolding. This novel observation reveals a direct role of α-Syn in causing genome damage and neuronal death in PD.

MATERIALS AND METHODS

Plasmid constructs

pcDNA-NES-α-Syn and pcDNA-NLS-α-Syn plasmids containing additional nuclear localization signal (NLS) or nuclear export signal (NES) sequences were a kind gift from Dr. Mel B. Feany (Harvard Medical School) [23]. Inducible mammalian FLAG-α-Syn expression vector was generated by cloning blunt-ended full-length α-Syn amplified from pcDNA-WT-α-Syn plasmid using Deep Vent DNA polymerase (M0258, NEB) into pCW-Cas9 vector (gift from Eric Lander and David Sabatini, Addgene plasmid 50661) [32] and digested with restriction enzymes NheI (R0131, NEB) and BamHI (R0136, NEB) followed by DNA polymerase I, large (Klenow; M0210, NEB) treatment to generate blunt ends. The primers used to amplify C-terminal FLAG-tagged α-Syn were as follows: forward primer, 5'-ATG GAT GTA TTC ATG AAA GGA CT-3'; reverse primer, 5'–CAC TGT CGA CTT ACT TAT CGT CAT CGT CTT TGT AAT CGG CTT CAG GTT CGT AGT CTT GAT ACC-3'.

Cell culture and treatments

The human neuroblastoma SHSY-5Y line was routinely maintained in regular Dulbecco's Modified Eagle's Medium (DMEM) supplemented with 10% fetal bovine serum (FBS; Gibco) and 1% penicillin/streptomycin (Corning). Transfection of SHSY-5Y cells with pcDNA-NES-α-Syn, pcDNANLS-α-Syn, and pCW-FLAG-α-Syn plasmids was carried out using Lipofectamine 2000 (Invitrogen) according to the manufacturer's instructions. NLS- and NES-tagged α-Syn plasmid-transfected cells were selected with antibiotic G418 sulphate (Corning), and doxycycline (Dox)-inducible α-Syn-expressing cells were selected against the antibiotic puromycin (InvivoGen) with a dose of 10 μg/mL.

Dox (5 μg/mL for 0, 24, 48, or 72 h)-inducible (i) FLAG-α-Syn levels were optimized for 2–3-fold overexpression. The cells were treated with $FeSO_4$ (200 μM) or $CuSO_4$ (200 μM) in DMEM supplemented with 1% FBS media for 24 h.

Human iPSC culture and generation of neural progenitor cells (NPC)

A control iPSC line KYOU-DXR0109B (201B7) was obtained from ATCC and grown in CellMatrix basement membrane gel (ACS-3035) and Pluripo-tent Stem Cell SFM XF/FF

media (ACS-3002) at 37°C and 5% CO_2. The iPSC line (ND34391*H) with α-Syn *SNCA* gene triplication (*SNCA*-tri) was obtained from the CORIELL Institute cell repository. *SNCA*-tri iPSCs were initially grown in 0.1% gelatin-coated 6-well plates covered with γ-irradiated CF-1 mouse embryonic fibroblasts and DMEM/F12 20% knock-out serum replacement (Gibco 11330–032, 10828010). At passage 3, *SNCA*-tri iPSCs were transitioned into a feeder-free system and maintained in a CellMatrix-coated dish and Essential 8 medium (E8M; Gibco A1517001). Derivation of NPCs from both control and *SNCA*-tri iPSCs was done using PSC neural induction medium (Gibco A1647801) as per the manufacturer's protocol. Briefly, E8M was replaced with neural induction medium approximately 24 h after passaging iPSCs, which were maintained in this medium for 7 days. Then the NPCs (P0) were passaged onto Geltrex (Thermo Fisher)-coated 6-well plates and expanded in StemPRO neural stem cell SFM media (A1050901). Neural induction efficiency was determined at passage 3 by immunofluorescence staining with a pluripotent marker (Oct4) and neural lineage stem cell marker (Nestin).

Real Time-PCR analysis for α-Syn mRNA quantitation

Total RNA was isolated using RNeasy Mini Kit (Qiagen #74104) following the manufacturer's protocol. Two microgram RNA was used for cDNA synthesis in a 20 μL reaction using SuperScript III reverse transcriptase kit (Invitrogen, #18080–044). α-Syn expression in the samples were analyzed by SYBR GREEN-based Real Time PCR (7000 Real-Time PCR System; Applied Biosystems) using SYBR Premix Ex Taq (TaKaRa) and primers appropriate for α-Syn expression described in [33] (HaSynTfw 5'-AGG GTG TTC TCT ATG TAG G-3' HaSynTrv 5'-ACT GTC TTC TGG GCT ACT GC) and HPRT1 expression (internal control; primer sequences: RealTimePrimers.com). Data were represented as fold change mRNA expression with respect to the reference samples set at 1 based on $2^{-\Delta\Delta CT}$ method.

Electrophoresis and immunoblotting

Whole cell protein extracts were obtained by harvesting the cells in ice-cold phosphate-buffered saline (PBS) and lysing them with STEN lysis buffer (50 mM Tris-HCl (pH 7.6), 150 mM NaCl, 0.1% SDS, 1% Nonidet P-40, 2 mM EDTA, and protease inhibitor) on ice for 20 min. Cytoplasmic and nuclear fraction protein were obtained by first lysing the harvested cells in cytoplasmic buffer (10 mM Tris-HCl (pH 7.9), 0.34 M sucrose, 3.0 mM $CaCl_2$, 2.0 mM $MgCl_2$, 0.1 mM EDTA, 1 mM DTT, 0.1% Nonidet P-40, and protease inhibitor) on ice for 10 min followed by centrifugation at 3500 g for 15 min at 4°C. Supernatant was collected as the cytoplasmic fraction, and the pellet was lysed with nuclear lysis buffer (20 mM HEPES (pH 7.9),3.0 mM EDTA, 10% glycerol, 150 mM potassium acetate, 1.5 mM $MgCl_2$, 1 mM DTT, and 0.5% Nonidet P-40), vortexed for 15 min at 4°C, and centrifuged at 16000 g for 10 min at 4°C. Protein content was estimated using the Bradford method (Bio-Rad).

Gel electrophoresis was performed as described previously [34, 35]. Protein samples were prepared for electrophoresis by dilution with their corresponding lysis buffers and addition of 4 × NuPAGE LDS samples; samples were not subjected to boiling. If not stated otherwise, 30 μg protein was loaded per lane in NuPAGE 4–12% Bis-Tris gel and

electrophoresed with NuPAGE MES-SDS running buffer. Gels were then electroblotted onto Immobilon-PSQ 0.45-μm PVDF membranes (Millipore) for 3 h at 30 V constant current at 4°C in 1 × Tris-Glycine solution (Fisher Scientific) and 20% methanol transfer buffer. After transfer, membranes were fixed with 0.4% paraformaldehyde (PFA) in PBS for 30 min at room temperature (RT), followed by blocking in 5% skim milk in TBS-T. The membranes were incubated with primary antibody diluted in 1% skim milk in TBST for 1 h at RT or overnight at 4°C, followed by washing in 1 × TBS-T and then incubation with secondary antibody for 1 h at RT and development with SuperSignal West Pico Chemiluminescent Substrate (Thermo Fisher).

Proximity ligation assay (PLA)

About 20,000 cells were seeded per well in 8-well chamber slides (Millipore) and grown for 2 days with Dox (5 μg/mL) induction. After the indicated treatment, the cells were fixed with 4% PFA for 15 min in the dark at RT, permeabilized in 0.2% Triton X-100 (Sigma) in 1× PBS for 10 min at RT, washed with PBS, blocked with 100 mM glycine, and washed again with PBS. The *in situ* PLA experiment was performed using the DuoLink kit (Olink Biosciences, Uppsala, Sweden) following the manufacturer's instructions. The following primary antibodies were used at the specified dilutions: mouse anti-FLAG at 1:1000; rabbit anti-α-Syn at 1:200, and rabbit anti-histone 3 at 1:200 dilution. The nuclear background of cells was visualized by staining with 4',6-diamidino-2-phenylindole (DAPI; Agilent Technologies). After staining, cells were examined with a Zeiss Axio Observer 7 microscope.

Chromatin immunoprecipitation (ChIP) assay

ChIP analysis was performed following the procedure described previously [36–38]. Briefly, cells in 10-cm plates were washed with PBS, cross-linked with 1% formaldehyde, lysed, and sonicated (XL-2000; QSonica LLC). IP was then performed in the cleared lysate with 5 μg of FLAG antibody (Sigma, for FLAG-α-Syn) or control IgG (Santa Cruz Biotechnology, Inc.) and Magna ChIP Protein A magnetic beads (Millipore, catalog no. 16–661) overnight. After washing the IP beads, protein-DNA complexes were eluted and the cross-links were reversed. DNA was purified using standard phenol/chloroform extraction and finally dissolved in 10 mM Tris-HCl (pH 8). The ChIP and 1% of the input DNA were subjected to SYBR Green-based real-time PCR (7500 Real-Time PCR System; Applied Biosystems) with appropriate primers (Supplementary Table S1) and SYBR Premix Ex Taq (TaKaRa). ChIP data were calculated as percent input.

Biotin affinity co-elution

For affinity co-elution assay, a 50-bp, 5'-biotin-tagged oligo and its complementary oligo were purchased from Sigma. The oligos were annealed by gradual cooling in a boiling water bath to generate a duplex oligo. Biotinylated dsOligo at a final concentration of 10 μM was mixed with 1 μg recombinant α-Syn (rPeptide) or 1 μg whole cell extract from SHSY-5Y cells ectopically expressing α-Syn or 1 μg purified BSA as a negative control in PBS and incubated at 30°C for 15 min with gentle shaking. The affinity pull-down was performed with Streptavidin-coupled Dynabeads™ M-280 (Thermo Scientific) following the manufacturer's protocol. The eluted protein product was tested by immunoblotting.

Oxidation of α-Syn by singlet oxygen

Singlet oxygen ($^1O_2$) was generated by irradiating riboflavin (Sigma R9504) solution (1% PBS) with UVB (UVP UVLMS-38). Recombinant α-Syn (2 μg) was added to the irradiated solution and incubated for 1 h followed by addition of supercoiled (sc) plasmid DNA for 4 h. To test oxidized α-Syn-mediated DNA strand breaks *in cell*, UVB-irradiated riboflavin solution containing recombinant α-Syn was added to the cell culture media for 4 h followed by DNA strand break analysis by Comet assay.

Comet assay

Alkaline Comet assay was performed using Trevigen's Comet assay kit (#4250–050-K). Briefly, Dox-induced cells and empty vector cells treated with and without metals were lysed, resuspended in low melting agarose, and spread evenly onto Comet slides. The slides were immersed in freshly prepared alkaline unwinding solution prior to alkaline electrophoresis. DNA in the nucleoid was visualized with SYBR Gold staining using an EVOS FL auto-fluorescence microscope (Life Technologies). Comet tail moment was scored using the Open Comet plugin for ImageJ software with 50 randomly selected cells.

Long amplicon (LA)-polymerase chain reaction (PCR)

After exposure to redox metals for 24 h, iFLAG-α-Syn SHSY5Y cells, *SNCA*-tri iPSCs, and respective controls were harvested for genomic DNA isolation using DNeasy blood and tissue kit (Qiagen #69504) as per the manufacturer's instructions. Genome integrity was assessed using LongAmp *Taq* DNA polymerase (NEB) to amplify a 10.4 kB region of the *HPTR* gene with the following primers: 5'-TGG GAT TAC ACG TGT GAA CCA ACC-3' and 5'-GCT CTA CCC TCT CCT CTA CCG TCC-3' [39]. PCR was performed at 94°C for 3 min followed by 25cycles at 94°C for 30 s, 58°C for 40 s, and 65°C for 10 min, and a final elongation step for 15 min. A small region (250 bp) of the *HPRT* gene was amplified using Jump-Start RedTaq DNA polymerase (Sigma) to normalize amplification obtained from the large fragment using the following primers: 5'-TGC TCG AGATGT GAT GAA GG-3' and 5'-CTG CAT TGT TTT GCC AGT GT-3' [40]. All amplified products were separated by electrophoresis in 0.8% agarose gel and stained with ethidium bromide. Relative DNA amplification percentage was calculated by gel band density analysis using ImageJ software or Pico Green dsDNA assay (Invitrogen, p7589).

Immunofluorescence

pCW-iFLAG-α-Syn SHSY-5Y cells were grown on 8-well chamber slides. Slides for iPSCs and NPCs were coated with Matrigel and Geltrex, respectively. Cells were fixed by replacing the media with fresh media and adding 8% PFA in PBS, obtaining a 4% PFA solution. Slides were then permeabilized with 0.2% Triton 100X in 1X PBS and blocked with 3% BSA-PBS-T (1 × PBS with 0.1% Tween-20) and incubated with primary antibody for α-Syn EP1646Y (Novus Biologicals) and anti-DDK (Origene Clone 4CS TA50011). After incubation with Alexa Fluor 488 (green)- and 558 (red)-conjugated secondary antibodies, coverslips were mounted in DAPI (Sigma). Images were taken using an Olympus BX61-Regular Upright BF & Fluorescent/Reflect Microscope using a 60 × objective.

Thioflavin T (Thio T) fluorescence

Recombinant α-Syn was incubated in 0.01 M Tris-HCl (pH 7.4) at 37°C with vigorous stirring with a magnetic bar in glass vials. Aliquots were removed from the incubation mix at the indicated time intervals and diluted to appropriate concentrations for Thio T fluorescence measurements to assess the formation of protein aggregates. Fluorescence was measured using a HITACHI 2000 spectrofluorimeter from the emission spectra (470–650 nm) with excitation at 450 nm using a 5-nm band pass for both excitation and emission.

For DNA cleavage analysis *in vitro*, aliquots of α-Syn (1 μM) from the aggregation reaction were mixed with 0.1 μg plasmid scDNA (pUC19) and incubated at 37°C for 4 h before being separated by 1% agarose gel electrophoresis.

Quantification of DNA strand breaks

Single-strand breaks (SSBs) were quantified using a nick translation reaction with *E. coli* DNA polymerase I (Klenow Fragment), which adds nucleotides at the 3'-OH end of an SSB [41]. When one of the dNTPs is P^{-32}-labeled, the incorporation of radioactivity is proportional to the number of SSBs present in the DNA. The 50 μL reaction mixture consisted of 40 mM Tris-HCl (pH 8.0), 1 mM β-mercaptoethanol, 7.5 mM $MgCl_2$, 4 mM ATP, 100 μM each of dATP, dCTP, and dGTP, 25 μM dTTP, 1 μCi ^{3}[H]TTP, 1 μg plasmid scDNA, and 1 unit of *E. coli* DNA polymerase I together with the indicated amounts of α-Syn.

Double-strand breaks (DSBs) were quantified by a terminal transferase based assay [42]. Terminal deoxynucleotidyl transferase catalyzes the addition of deoxynucleotides to the 3' termini of DNA at the blunt end. Similar conditions were used to incubate DNA with terminal transferase, as in the case of *E. coli* polymerase I assay. The incorporation of ^{3}[H]-dTTP into DNA is proportional to the number of DSBs in the DNA. DNA breaks were quantified with reference to a control DNA with a known number of breaks as described previously [43].

Circular dichroism (CD) studies

CD spectra (190–300 nm) were recorded on a JASCO J-700 spectropolarimeter for aliquots of α-Syn withdrawn from aggregation reactions at various time intervals. The protein was diluted to a final concentration of 5 μM in 0.01 M Hepes buffer (pH 7.0). Each spectrum was the average of four repetitions. All spectra were corrected by subtraction from buffer spectra.

Flow-cytometric analysis of cell death

The levels of apoptosis in iFLAG-α-Syn cells ± Dox treatment after exposure to metal salts for 24 h was measured using the FITC Annexin V apoptosis detection kit I (BD Biosciences 556547). Flow-cytometric analysis of apoptotic cell death was performed as indicated earlier [44]. Briefly, cells were harvested, washed with PBS, and incubated with fluorescein isothiocynate (FITC) conjugated Annexin V and propidium iodide (PI) according to the instruction of Annexin V apoptosis detection kit. A total of 10,000 events were acquired per sample by fluorescence activated cell sorting (FACS) and analyzed using Flowjo software

(Becton-Dickinson Biosciences, San Jose, CA). Unstained and single fluorochrome controls were used for background subtraction (data not shown).

Reactive oxygen species (ROS) measurement in live cells

CellROX green reagent (Life Technologies C10492), a dye that binds to DNA upon oxidation, was used to assess ROS accumulation in iFLAG-α-Syn SHSY-5Y cells ± Dox exposed for 24 h to Fe/Cu salts. After treatment, cells were stained with Cell-ROX green following the manufacturer's protocol. The data from FACS acquisition was analyzed using Flowjo software.

Statistical analysis

Graphpad prism 6 software was used for data analysis. Comparisons of groups were generated with two-way Anova followed by Sidak's or Tukey's multiple comparison test to compare selected pair of means. *p*-values are indicated in the associated figure legends.

RESULTS

Chromatin association of nuclear α-Syn and its physical binding to naked DNA in vitro

Despite compelling evidence for the binding of α-Syn to DNA oligos *in vitro*, there are conflicting reports in the literature concerning the presence and role of α-Syn in neuronal nuclei, particularly in PD condition. The difficulty in establishing the presence of nuclear α-Syn appears primarily due to its predominantly cytosolic localization in presynaptic nerve terminals and the presence of a relatively low fraction (<5%) of the protein in the nuclear compartment under normal conditions. To conclusively test α-Syn localization and its interaction with chromatin, we generated a Dox-inducible FLAG-α-Syn-expressing SHSY-5Y cell line (pCW-iFLAG-α-Syn SHSY-5Y line) allowing ectopic expression of α-Syn in a controlled and reproducible fashion. Dox treatment (5 μg/mL) for 72 h gradually increased both ectopic FLAG-α-Syn and total α-Syn levels in the pCW-iFLAG-α-Syn SHSY-5Y line (Fig. 1A). A ~ 2- to 3-fold increase in total α-Syn level was consistently observed at 72 h after Dox induction. Immunofluorescence using FLAG or α-Syn antibody showed significant nuclear localization of α-Syn with an increase in its expression, as indicated in the enlarged image acquired at 72 h of Dox induction (Fig. 1B). We then utilized modified PLA, which is a highly sensitive for *in situ* detection of protein-protein interaction in cells [45]. Here, instead of two antibodies for different proteins used in typical PLA, we used FLAG versus α-Syn antibodies in the pCW-iFLAG-α-Syn SHSY-5Y line to detect ectopic α-Syn. A number of nuclear PLA foci within DAPI-stained regions confirmed the presence of FLAG-α-Syn in the nuclei (Fig. 1C, top). We then examined the association of α-Syn with chromatin. Strong PLA signals for FLAG versus histone H3 antibodies showed α-Syn binding to H3 in the chromatin (Fig. 1C, bottom).

To further confirm the chromatin association of α-Syn, we performed chromatin immunoprecipitation (ChIP) using FLAG antibody in pCW-iFLAG-α-Syn SHSY-5Y cells and then PCR-amplified the purified ChIP DNA with a set of four randomly selected primer pairs. These primers targeted proximal (–165/+82; promoter region) and distal (–72987/–72800) regions of the RARβ2 gene and a randomly selected segment within chromosome 17

that does not harbor any gene signature, and the HPRT gene. Relatively high amplification of proximal RARβ2 promoter region was observed compared to its distal region, or the non-gene region in chromosome 17 (Fig. 1D, Supplemental Figure 1A). Moderately high binding was also observed for HPRT gene (Supplementary Figure 1B). These data not only suggested an association between α-Syn and chromatin but also indicated the possible functional binding of α-Syn to distinct chromosomal regions containing specific genes. However, we decided to pursue the functional implications of distinct and specific chromatin binding of α-Syn in a separate study and focus on the general pathological impact of α-Syn toxicity on neuronal genomes in the present study. Furthermore, we tested whether α-Syn binds to naked DNA *in vitro* using a biotin affinity co-elution analysis. Immunoblotting revealed that both recombinant α-Syn (Rec.α-Syn) and α-Syn in the SHSY-5Y nuclear extract co-eluted with a biotin-tagged duplex oligonucleotide (Fig. 1E). Together, these data demonstrate that α-Syn binds to DNA and chromatin both in cells and *in vitro*.

α-Syn expression induces strand breaks in the neuronal genome synergistically with Fe

The evidence for the presence of extensive genome damage in PD-affected human brains and various PD model systems [29–31] led us to examine DNA breaks in α-Syn-overexpressing cells in presence of pro-oxidant Fe or Cu salts. Fe has been shown to accumulate in α-Syn-rich Lewy bodies in the PD brain and within α-Syn-rich inclusions in PD neuronal cells [6, 46]. Alkaline Comet assay of the pCW-iFLAG-α-Syn SHSY-5Y line showed a pronounced increase in mean comet tail moment 48 h after Dox induction, which was further enhanced in $FeSO_4$-treated cells (Fig. 2A, B). Five-fold increase in genome damage was caused by ~2-fold induction of α-Syn. The presence of $FeSO_4$ resulted in about an 8-fold increase in strand breaks in α-Syn-overexpressing cells. Unlike $FeSO_4$, which showed synergistic toxicity when combined with α-Syn, $CuSO_4$ showed only an additive effect. A similar dose of $FeSO_4$ and $CuSO_4$ exposure in uninduced pCW-iFLAG-α-Syn SHSY-5Y cells caused only moderate (<2-fold) increase in the mean comet tail moment. LA-PCR analysis of the genomic DNA isolated from the above cells confirmed marked reduction in genomic integrity in Fe-treated, α-Syn-overexpressing cells (Fig. 2C, D). Amplification of a 10.4 kb and a shorter 250 bp region within the *HPRT* gene followed by agarose gel electrophoresis (Fig. 2C) and gel band density-based quantification (Fig. 1D) showed 30% decrease in amplified product in α-Syn-overexpressing cells. A reduction in amplified product in LA-PCR indicates the presence of strand breaks within the amplified region [39]. Consistent with Comet analysis, a further 45% and 70% decrease was observed in $CuSO_4$ and $FeSO_4$-treated cells, respectively (Fig. 2C, D). Similarly, addition of recombinant α-Syn to cultured SHSY-5Y cells combined with Fe cooperatively induced extensive DNA damage (Supplementary Figure 2).

Nuclear but not cytosolic α-Syn induces neuronal genome damage

To test the direct role of nuclear α-Syn in causing genome damage, we transiently transfected SHSY-5Y cells with mutant α-Syn expression vectors containing additional NLS or NES sequences. Immunofluorescence (Fig. 3A) and immunoblotting (Fig. 3B) confirmed the nuclear- and cytosolic expression of NLS-α-Syn and NES-α-Syn, respectively. Comet analysis showed about 2-fold higher mean tail moment for NLS-α-Syn-expressing cells compared with WT-α-Syn or NES-α-Syn cells (Fig. 3C, D). The damage was further

enhanced after Fe or Cu treatment in NLS-α-Syn and WT-α-Syn cells but not in NES-α-Syn cells. These data thus demonstrate that the nuclear localization of α-Syn is required for inducing genome damage in neurons.

DNA nicking activity of α-Syn is enhanced by misfolding/oligomerization.

We next examined the effect of α-Syn binding on plasmid scDNA using recombinant protein *in vitro*. Separation of plasmid DNA by agarose gel electrophoresis after incubation with α-Syn for 12 h showed conversion of the scDNA form into a mixture of open circular and linear forms together with shorter sheared fragments (Fig. 4A). Quantification of breaks in plasmid DNA using a nick translation method [29, 43] showed 6-fold increase in SSBs but only a moderate increase in DSBs (Fig. 4B).

We then correlated the misfolding/aggregation of α-Syn with its DNA nicking activity. Aliquots of α-Syn incubated with constant stirring for promoting aggregation, as monitored by Thio T fluorescence (Fig. 4C), were mixed with scDNA, and strand breaks were quantified by agarose gel (Fig. 4D) and nick translation (Fig. 4E). Interestingly, the misfolded or early oligomeric α-Syn indicated by CD spectroscopy (Fig. 4F) caused higher DNA damage compared with monomeric or aggregated forms. This is again consistent with the model of higher toxicity of α-Syn oligomers [47].

Oxidation of α-Syn may promote its DNA nicking activity

α-Syn has been shown to oxidize in PD conditions [13]. Based on this previous observation and the enhancement of DNA nicking activity by α-Syn-pro-oxidant metal complex in our study, we suspected that the oxidized form of α-Syn might mediate DNA cleavage. To test this possibility, we exposed riboflavin with UVB to generate $^1O_2$ before incubation with α-Syn for 1 h followed by mixing with scDNA. Agarose gel electrophoresis showed significant shearing of DNA by oxidized α-Syn compared with WT-α-Syn or $^1O_2$-treated DNA (Fig. 5A). We then treated SHSY-5Y cells with WT- or oxidized α-Syn and quantified genome damage by Comet analysis (Fig. 5B). Consistent with the *in vitro* data, an ~5-fold higher mean tail moment was observed with oxidized α-Syn versus a 2-fold increase with WT-α-Syn. These data suggest that oxidized α-Syn is critical for inducing genome damage. Similar chemical nuclease activity of short oxidized peptides containing oxidizable Tyr or Thr residues together with basic residues has been previously characterized [48]. These peptides extract protons from phosphodiester bonds in the DNA backbone to nick DNA. It is likely that α-Syn-mediated genome damage involves a similar chemical nicking mechanism.

Fe-dependent ROS generation after α-Syn induction in neurons

We observed a significant increase in ROS-positive cells after α-Syn in the presence of $FeSO_4$ but not in the presence of $CuSO_4$ (Fig. 6A, B). Fluorescence microscopy revealed increased α-Syn aggregate formation in the perinuclear region of FLAG-α-Syn-overexpressing cells exposed to $FeSO_4$ (Fig. 6C). However, the negligible increase in ROS with $CuSO_4$ was surprising but is likely due to activation of Cu/Zn superoxide dismutase by Cu to quench ROS [49].

α-Syn-induced genome damage in NPC lines derived from PD patient iPSC cells

Given that a small pool of neural stem cells are a potential source for replacing degenerated neurons in PD patients [50], we generated NPC lines from a normal or PD patient–derived SNCA-tri iPSC cells and characterized the NPCs with appropriate markers (Fig. 7A–C). The SNCA-tri iPSC line possesses SNCA gene triplication and thus shows ~3-fold overexpression in α-Syn levels and up to ~5-fold overexpression upon conversion to NPC, as confirmed by immunofluorescence (Fig. 7C) and mRNA quantitation by RT-PCR (Fig. 7D), consistent with previous studies [51]. DNA damage analysis by LAPCR showed presence of significantly higher number of DNA strand breaks in SNCA-tri NPC cells compared to control NPC cells (Fig. 7E), as indicated by ~30% reduced amplification of HPRT gene long amplicon quantified using Pico Green dsDNA assay (Fig. 7F). Exposure to 200 μM $FeSO_4$ synergistically increased DNA damage in SNCA-tri NPC cells over the control. The moderate synergy of Fe in SNCA-tri NPC cells (Fig. 7 E, F) over transiently induced α-Syn in pCW-iFLAG-α-Syn SHSY-5Y line (Fig. 2) may be attributed to the constitutive overexpression of α-Syn in SNCA-tri NPC line, which may sequester cellular Fe. On the other hand, $CuSO_4$ induced DNA damage is comparable to that in Fe-treated NPC cells, unlike in SHSY-5Y cells, presumably due to their differential antioxidant capacity. Furthermore, treatment of control NPC cells with 300 nM recombinant α-Syn together with 200 μM $FeSO_4$ resulted in a ~ 22% reduction in HPRT gene amplification product (Supplementary Figure 2B).

α-Syn and Fe cooperatively induce neuronal apoptosis

To further address the Fe-dependent neurotoxicity of α-Syn, we performed Annexin V-FITC/PI dual staining pCW-iFLAG-α-Syn SHSY-5Y cells with or without Fe/Cu. The cells were induced for 48 h with Dox, which resulted in ~12% increase in early (Q3) and late (Q2) apoptotic cell population. Both un-induced and induced cells were then exposed to $FeSO_4$ or $CuSO_4$. A 4–8% cell population migrated directly from Q1 to Q4 in un-induced cells after Fe/Cu treatment, which presumably represents a combination of necrosis and ferroptosis [52, 53] (Fig. 8A). However, Fe caused a significant increase (~ 16%) in early and late apoptotic cells (quantitated from Q2 and Q3, respectively) in Dox-induced cells (Fig. 8A, B). CuSO4 did not affect α-Syn-mediated neuronal apoptosis in Dox-induced cells. Interestingly, Fe- or Cu- induced necrosis or possible ferroptosis (Q4) observed in un-induced cells was prevented after α-Syn induction. This is likely due to sequestration of free metal ions by overexpressed α-Syn, preventing metal mediated necrosis/ferroptosis.

DISCUSSION

Our results demonstrate novel DNA cleavage activity of α-Syn both *in vitro* and in genomes of cultured neurons. This activity was upregulated in the presence of pro-oxidant Fe as well as $^1O_2$. We first established that nuclear-localized α-Syn binds to distinct DNA sequences in the chromatin and physically binds naked DNA *in vitro*. To gain further molecular insights into α-Syn's DNA binding and nicking activity, we used MD simulation with nucleic acid-protein docking method (NPDock) [54] to predict the three-dimensional structure of the α-Syn-DNA complex (Fig. 9 and Supplementary Figure 3). The DNA was predicted to interact with the positively charged lysine-rich repeat motifs (KTKEGV) located predominantly in

the N-terminus and partly in the central domains of the α-Syn sequence. The DNA is highly unlikely to bind to the C-terminal end of α-Syn, which is rich in negatively charged residues. Consistently, previous studies show that α-Syn has a propensity to form broken helices in the N-terminal region owing to the presence of several 11 amino acid repeats that may form a helix-turn-helix type of motif that is commonly present in many classical DNA-binding proteins [55, 56]. After α-Syn's initial electrostatic interaction with the DNA backbone, subtle conformational change in α-Syn, induced by its oxidation or by Fe, could stabilize the interaction facilitating DNA nicking activity. In cells, however, α-Syn interaction with histone proteins (Fig. 1C) may contribute to the initial chromatin binding.

Although α-Syn is primarily a presynaptic nerve terminal protein that is predominantly enriched in the membrane, several studies show the presence of α-Syn in neuronal nuclei [18, 21, 23, 24]. However, the functional or pathological implications of nuclear α-Syn are unclear. Ma et al. suggest that residues (103–140) located at the C-terminus of α-Syn are critical for its nuclear localization [22]. They have also proposed involvement of importin α, a nuclear-transport receptor protein, in the translocation of α-Syn into the nucleus. Although no direct interaction between α-Syn and importin α was observed, the authors suggest the involvement of other proteins mediating complex formation. Another recent study reported the role of a tripartite motif-containing protein 28 (TRIM28) in stabilizing α-Syn in the neuronal nucleus [25]. TRIM28 contains an NLS sequence that interacts with various importin α subtypes, facilitating its nuclear import where it binds to chromatin [57, 58]. TRIM28, along with importin α, may thus play a role in α-Syn's nuclear import, which should be further investigated. Moreover, under PD condi tions, α-Syn nuclear localization is likely enhanced due to non-specific transportation through the oxidatively damaged nuclear membrane [11]. Recent studies showed that overexpressed α-Syn accumulates in the perinuclear region, which is consistent with our findings. Cells exposed to Fe have been found to present Fe-rich α-Syn inclusions within the perinuclear regions [46]. Interestingly, Fe has also been found to disrupt the nuclear membrane, allowing perinuclear α-Syn to translocate into disrupted nuclei [59]. Thus, both physiological and pathological conditions could favor α-Syn's nuclear localization in PD-affected neurons.

The fact that increased oxidative stress and Fe accumulation are hallmarks of the PD brain, led us to investigate the impact of these conditions on α-Syn-DNA interaction. We observed that α-Syn overexpression combined with Fe exposure or oxidative stress significantly enhanced DNA damage in the neuronal genome. Furthermore, genome damage was dependent on nuclear α-Syn as determined by the expression of NLS or NES mutants. On the other hand, cytosol-specific α-Syn expression inhibited DNA breaks formation even in the presence of metal salts, likely due to their sequestration by oligomeric α-Syn. Furthermore, the enhanced DNA nicking activity of α-Syn after its exposure to $^1O_2$ or Fe, suggests that oxidized α-Syn is involved in causing DNA strand-breaks, likely by acting as a chemical nuclease. It was previously shown that when surrounded by basic residues, peroxides of Trp, Tyr, Met, Asp, Pro, and Cys in proteins formed by ROS and/or transition metals, acquire DNA strand cleavage activity, by abstracting a proton from the phosphodiester linkage, causing its cleavage [48]. It is likely that a similar mechanism is involved in α-Syn induced DNA damage. Fe ions could contribute to α-Syn oxidation via their binding to oxidation prone residues such as Met, Cys, Thr, Tyr, and Trp in α-Syn.

Interestingly, we found that the DNA cleavage level was the highest with misfolded/oligomeric α-Syn, suggesting that exposure of oxidation-prone regions may be critical. We propose that blocking oxidation prone peptide sequence in combination with metal chelators could be an effective therapeutic strategy, which we are currently investigating. In cells, α-Syn folding could be promoted by accumulated redox active metal ions, as was reported by our lab [60, 61] and others [9, 10]. In addition to α-Syn, Aβ, tau and prion proteins implicated in AD and prion diseases, also have DNA binding activity, suggesting that DNA binding is a common property of many amyloidogenic proteins associated with various neurodegenerative disorders [28, 62–64]. However, the role of their DNA binding in disease pathology has not been well studied.

In addition to Fe, previous studies have showed that α-Syn binds Cu *in vitro*. Cu was shown to bind the ^{1}MVDFM^{5} motif in the α-Syn N-terminus and promote its oligomerization [14]. However, our in cell data show no synergistic neurotoxicity or genome damage by α-Syn and Cu. This raises the question about the *in vivo* relevance of toxicity of Cu-α-Syn complex for PD. Unlike the available compelling evidence for Fe accumulation, Cu has not been consistently shown to accumulate in the PD brain, nor in Lewy body inclusions. Furthermore, Cu at low concentrations could activate superoxide dismutase, and thus may protect cells from ROS toxicity [49]. Although both Fe and Cu are redox-active, they have the distinct ability to affect α-Syn-mediated neurotoxicity. Furthermore, Fe and Cu caused a small but subtle increase in non-apoptotic cell death (Q1 to Q4 migration in Fig. 8) in cultured neurons in the absence of α-Syn, which was prevented by α-Syn overexpression, although apoptotic cell population increased. While the nature of this direct metal induced cell death is not clear, it is possible that both necrosis and recently discovered ferroptosis [52] contributes to the pathway triggered by direct exposure to free metals in cultured cells that lack robust metal storage/sequestration machinery. Recent studies show that activation of ferroptosis plays a role in the nonapoptotic destruction of cancer cells, but its inhibition may protect from neurodegeneration. The prevention of such non-apoptotic cell death after α-Syn induction suggests that moderate increase in α-Syn may be protective against Fe-induced ferroptosis, which should be the subject of future investigation.

It is important to note that α-Syn primarily forms SSBs in DNA. However, with prolonged incubation with α-Syn *in vitro*, DSBs were formed in plasmid DNA, presumably due to the accumulation of several SSBs in close proximity. A schematic representation of the DNA cleavage mechanism of α-Syn is shown in Fig. 10. Our studies thus highlight the role of α-Syn in inducing DNA cleavage and the contribution of ROS or pro-oxidant Fe/Cu to this process, which may have a profound impact on our approach to PD prevention and therapy.

Supplementary Material

Refer to Web version on PubMed Central for supplementary material.

ACKNOWLEDGMENTS

This research was supported by grants from the National Institutes of Health (USPHS R01 NS088 645), Muscular Dystrophy Association (MDA 294 842), Alzheimer's Association (NIRG-12–242135), and Houston Methodist Research Institute to M.L.H. and Melo Brain Funds to M.L.H. and K.S.R. V.V. is supported by a doctoral

scholarship from the Institute for Training and Development of Human Resources of Panama (IFARHU) and the National Secretariat for Science, Technology, and Innovation of Panama (SENACYT). K.S.R. is supported by the National System on Investigation grant of SENACYT. S.M. is supported by USPHS R01 GM105090. We thank Dr. Mel B. Feany (Harvard Medical School) for the kind gift of α-Syn NLS and NES expression plasmids.

Authors' disclosures available online (http://j-alz.com/manuscript-disclosures/17-0342r1).

REFERENCES

[1]. Theillet FX, Binolfi A, Bekei B, Martorana A, Rose HM, Stuiver M, Verzini S, Lorenz D, van Rossum M, Goldfarb D, Selenko P (2016) Structural disorder of monomeric α-synuclein persists in mammalian cells. Nature 530, 45–50. [PubMed: 26808899]

[2]. Raghavan R, de Kruijff L, Sterrenburg MD, Rogers BB, Hladik CL, White CL, 3rd (2004) Alpha-synuclein expression in the developing human brain. Pediatr Dev Pathol 7, 506–516. [PubMed: 15547775]

[3]. Narhi L, Wood SJ, Steavenson S, Jiang Y, Wu GM, Anafi D, Kaufman SA, Martin F, Sitney K, Denis P, Louis JC, Wypych J, Biere AL, Citron M (1999) Both familial Parkinson's disease mutations accelerate alpha-synuclein aggregation. J Biol Chem 274, 9843–9846. [PubMed: 10092675]

[4]. Singleton AB, Farrer M, Johnson J, Singleton A, Hague S, Kachergus J, Hulihan M, Peuralinna T, Dutra A, Nussbaum R, Lincoln S, Crawley A, Hanson M, Maraganore D, Adler C, Cookson MR, Muenter M, Baptista M, Miller D, Blancato J, Hardy J, Gwinn-Hardy K (2003) alpha-Synuclein locus triplication causes Parkinson's disease. Science 302, 841. [PubMed: 14593171]

[5]. Oczkowska A, Kozubski W, Lianeri M, Dorszewska J (2013) Mutations in PRKN and SNCA genes important for the progress of Parkinson's disease. Curr Genomics 14, 502–517. [PubMed: 24532983]

[6]. Hirsch EC, Brandel JP, Galle P, Javoy-Agid F, Agid Y (1991) Iron and aluminum increase in the substantia nigra of patients with Parkinson's disease: An X-ray microanalysis. J Neurochem 56, 446–451. [PubMed: 1988548]

[7]. Davies KM, Bohic S, Carmona A, Ortega R, Cottam V, Hare DJ, Finberg JP, Reyes S, Halliday GM, Mercer JF, Double KL (2014) Copper pathology in vulnerable brain regions in Parkinson's disease. Neurobiol Aging 35, 858–866. [PubMed: 24176624]

[8]. Sofic E, Lange KW, Jellinger K, Riederer P (1992) Reduced and oxidized glutathione in the substantia nigra of patients with Parkinson's disease. Neurosci Lett 142, 128–130. [PubMed: 1454205]

[9]. Peng Y, Wang C, Xu HH, Liu YN, Zhou F (2010) Binding of alpha-synuclein with Fe(III) and with Fe(II) and biological implications of the resultant complexes. J Inorg Biochem 104, 365–370. [PubMed: 20005574]

[10]. Rose F, Hodak M, Bernholc J (2011) Mechanism of copper(II)-induced misfolding of Parkinson's disease protein. Sci Rep 1, 11. [PubMed: 22355530]

[11]. Snead D, Eliezer D (2014) Alpha-synuclein function and dysfunction on cellular membranes. Exp Neurobiol 23, 292–313. [PubMed: 25548530]

[12]. Cole NB, Murphy DD, Lebowitz J, Di Noto L, Levine RL, Nussbaum RL (2005) Metal-catalyzed oxidation of alpha-synuclein: Helping to define the relationship between oligomers, protofibrils, and filaments. J Biol Chem 280, 9678–9690. [PubMed: 15615715]

[13]. Gao HM, Kotzbauer PT, Uryu K, Leight S, Trojanowski JQ, Lee VM (2008) Neuroinflammation and oxidation/nitration of alpha-synuclein linked to dopaminergic neurodegeneration. J Neurosci 28, 7687–7698. [PubMed: 18650345]

[14]. Miotto MC, Rodriguez EE, Valiente-Gabioud AA, Torres-Monserrat V, Binolfi A, Quintanar L, Zweckstetter M, Griesinger C, Fernandez CO (2014) Site-specific copper-catalyzed oxidation of α-synuclein: Tightening the link between metal binding and protein oxidative damage in Parkinson's disease. Inorg Chem 53, 4350–4358. [PubMed: 24725094]

[15]. Binolfi A, Limatola A, Verzini S, Kosten J, Theillet FX, Rose HM, Bekei B, Stuiver M, van Rossum M, Selenko P (2016) Intracellular repair of oxidation-damaged α-synuclein fails to target C-terminal modification sites. Nat Commun 7, 10251. [PubMed: 26807843]

[16]. Maroteaux L, Campanelli JT, Scheller RH (1988) Synuclein: A neuron-specific protein localized to the nucleus and presynaptic nerve terminal. J Neurosci 8, 2804–2815. [PubMed: 3411354]

[17]. Tanji K, Mori F, Imaizumi T, Yoshida H, Matsumiya T, Tamo W, Yoshimoto M, Odagiri H, Sasaki M, Takahashi H, Satoh K, Wakabayashi K (2002) Upregulation of alpha-synuclein by lipopolysaccharide and interleukin-1 in human macrophages. Pathol Int 52, 572–577. [PubMed: 12406186]

[18]. Goers J, Manning-Bog AB, McCormack AL, Millett IS, Doniach S, Di Monte DA, Uversky VN, Fink AL (2003) Nuclear localization of alpha-synuclein and its interaction with histones. Biochemistry 42, 8465–8471. [PubMed: 12859192]

[19]. Zhang L, Zhang C, Zhu Y, Cai Q, Chan P, Uéda K, Yu S, Yang H (2008) Semi-quantitative analysis of alpha-synuclein in subcellular pools of rat brain neurons: An immunogold electron microscopic study using a C-terminal specific monoclonal antibody. Brain Res 1244, 40–52. [PubMed: 18817762]

[20]. Lin BY, Kao MC (2015) Therapeutic applications of the TAT-mediated protein transduction system for complex I deficiency and other mitochondrial diseases. Ann N Y Acad Sci 1350, 17–28. [PubMed: 26273800]

[21]. Siddiqui A, Chinta SJ, Mallajosyula JK, Rajagopolan S, Hanson I, Rane A, Andersen JK (2012) Selective binding of nuclear alpha-synuclein to the PGC1alpha promoter under conditions of oxidative stress may contribute to losses in mitochondrial function: Implications for Parkinson's disease. Free Radic Biol Med 53, 993–1003. [PubMed: 22705949]

[22]. Ma KL, Song LK, Yuan YH, Zhang Y, Han N, Gao K, Chen NH (2014) The nuclear accumulation of alpha-synuclein is mediated by importin alpha and promotes neurotoxicity by accelerating the cell cycle. Neuropharmacology 82, 132–142. [PubMed: 23973294]

[23]. Kontopoulos E, Parvin JD, Feany MB (2006) Alpha-synuclein acts in the nucleus to inhibit histone acetylation and promote neurotoxicity. Hum Mol Genet 15, 3012–3023. [PubMed: 16959795]

[24]. Xu S, Zhou M, Yu S, Cai Y, Zhang A, Uéda K, Chan P (2006) Oxidative stress induces nuclear translocation of C-terminus of alpha-synuclein in dopaminergic cells. Biochem Biophys Res Commun 342, 330–335. [PubMed: 16480958]

[25]. Rousseaux MW, de Haro M, Lasagna-Reeves CA, De Maio A, Park J, Jafar-Nejad P, Al-Ramahi I, Sharma A, See L, Lu N, Vilanova-Velez L, Klisch TJ, Westbrook TF, Troncoso JC, Botas J, Zoghbi HY (2016) TRIM28 regulates the nuclear accumulation and toxicity of both alpha-synuclein and tau. eLife 5, doi: 10.7554/eLife.19809

[26]. Hegde ML, Jagannatha Rao KS (2003) Challenges and complexities of alpha-synuclein toxicity: Mew postulates in unfolding the mystery associated with Parkinson's disease. Arch Biochem Biophys 418, 169–178. [PubMed: 14522588]

[27]. Hegde ML, Rao KS (2007) DNA induces folding in alpha-synuclein: Understanding the mechanism using chaperone property of osmolytes. Arch Biochem Biophys 464, 57–69. [PubMed: 17537399]

[28]. Vasudevaraju P, Guerrero E, Hegde ML, Collen TB, Britton GB, Rao KS (2012) New evidence on α-synuclein and Tau binding to conformation and sequence specific GC* rich DNA: Relevance to neurological disorders. J Pharm Bioallied Sci 4, 112–117. [PubMed: 22557921]

[29]. Hegde ML, Gupta VB, Anitha M, Harikrishna T, Shankar SK, Muthane U, Subba Rao K, Jagannatha Rao KS (2006) Studies on genomic DNA topology and stability in brain regions of Parkinson's disease. Arch Biochem Biophys 449, 143–156. [PubMed: 16600170]

[30]. Yasuhara T, Hara K, Sethi KD, Morgan JC, Borlongan CV (2007) Increased 8-OHdG levels in the urine, serum, and substantia nigra of hemiparkinsonian rats. Brain Res 1133, 49–52. [PubMed: 17188662]

[31]. Wang D, Yu T, Liu Y, Yan J, Guo Y, Jing Y, Yang X, Song Y, Tian Y (2016) DNA damage preceding dopamine neuron degeneration in A53T human α-synuclein transgenic mice. Biochem Biophys Res Commun 481, 104–110. [PubMed: 27818201]

[32]. Wang T, Wei JJ, Sabatini DM, Lander ES (2014) Genetic screens in human cells using the CRISPR-Cas9 system. Science 343, 80–84. [PubMed: 24336569]

[33]. Rhinn H, Qiang L, Yamashita T, Rhee D, Zolin A, Vanti W, Abeliovich A (2012) Alternative α-synuclein transcript usage as a convergent mechanism in Parkinson's disease pathology. Nat Commun 3, 1084. [PubMed: 23011138]

[34]. Dettmer U, Newman AJ, Luth ES, Bartels T, Selkoe D (2013) In vivo cross-linking reveals principally oligomeric forms of α-synuclein and β-synuclein in neurons and non-neural cells. J Biol Chem 288, 6371–6385. [PubMed: 23319586]

[35]. Lee BR, Kamitani T (2011) Improved immunodetection of endogenous α-synuclein. PLoS One 6, e23939. [PubMed: 21886844]

[36]. Sengupta S, Mantha AK, Mitra S, Bhakat KK (2011) Human AP endonuclease (APE1/Ref-1) and its acetylation regulate YB-1-p300 recruitment and RNA polymerase II loading in the drug-induced activation of multidrug resistance gene MDR1. Oncogene 30, 482–493. [PubMed: 20856196]

[37]. Hegde PM, Dutta A, Sengupta S, Mitra J, Adhikari S, Tomkinson AE, Li GM, Boldogh I, Hazra TK, Mitra S, Hegde ML (2015) The C-terminal domain (CTD) of human DNA glycosylase NEIL1 is required for forming BERosome repair complex with DNA replication proteins at the replicating genome: DOMINANT NEGATIVE FUNCTION OF THE CTD. J Biol Chem 290, 20919–20933. [PubMed: 26134572]

[38]. Hegde ML, Hegde PM, Bellot LJ, Mandal SM, Hazra TK, Li GM, Boldogh I, Tomkinson AE, Mitra S (2013) Prereplicative repair of oxidized bases in the human genome is mediated by NEIL1 DNA glycosylase together with replication proteins. Proc Natl Acad Sci U S A 110, E3090–E3099. [PubMed: 23898192]

[39]. Kovalenko OA, Santos JH (2009) Analysis of oxidative damage by gene-specific quantitative PCR. Curr Protoc Hum Genet Chapter 19, Unit 19.1.

[40]. Sarker AH, Chatterjee A, Williams M, Lin S, Havel C, Jacob P, 3rd, Boldogh I, Hazra TK, Talbot P, Hang B (2014) NEIL2 protects against oxidative DNA damage induced by sidestream smoke in human cells. PLoS One 9, e90261. [PubMed: 24595271]

[41]. Mosbaugh DW, Linn S (1982) Characterization of the action of Escherichia coli DNA polymerase I at incisions produced by repair endodeoxyribonucleases. J Biol Chem 257, 575–583. [PubMed: 6273443]

[42]. Deng G, Wu R (1983) Terminal transferase: Use of the tailing of DNA and for in vitro mutagenesis. Methods Enzymol 100, 96–116. [PubMed: 6312266]

[43]. Mandavilli BS, Rao KS (1996) Accumulation of DNA damage in aging neurons occurs through a mechanism other than apoptosis. J Neurochem 67, 1559–1565. [PubMed: 8858940]

[44]. Pandey A, Vishnoi K, Mahata S, Tripathi SC, Misra SP, Misra V, Mehrotra R, Dwivedi M, Bharti AC (2015) Berberine and curcumin target survivin and STAT3 in gastric cancer cells and synergize actions of standard chemotherapeutic 5-fluorouracil. Nutr Cancer 67, 1293–1304. [PubMed: 26492225]

[45]. Fredriksson S, Gullberg M, Jarvius J, Olsson C, Pietras K, Gustafsdóttir SM, Ostman A, Landegren U (2002) Protein detection using proximity-dependent DNA ligation assays. Nat Biotechnol 20, 473–477. [PubMed: 11981560]

[46]. Ortega R, Carmona A, Roudeau S, Perrin L, Dučić T, Carboni E, Bohic S, Cloetens P, Lingor P (2016) α-synuclein over-expression induces increased iron accumulation and redistribution in iron-exposed neurons. Mol Neurobiol 53, 1925–1934. [PubMed: 25833099]

[47]. Winner B, Jappelli R, Maji SK, Desplats PA, Boyer L, Aigner S, Hetzer C, Loher T, Vilar M, Campioni S, Tzitzilonis C, Soragni A, Jessberger S, Mira H, Consiglio A, Pham E, Masliah E, Gage FH, Riek R (2011) In vivo demonstration that alpha-synuclein oligomers are toxic. Proc Natl Acad Sci U S A 108, 4194–4199. [PubMed: 21325059]

[48]. Prestwich EG, Roy MD, Rego J, Kelley SO (2005) Oxidative DNA strand scission induced by peptides. Chem Biol 12, 695–701. [PubMed: 15975515]

[49]. Qian Y, Zheng Y, Abraham L, Ramos KS, Tiffany-Castiglioni E (2005) Differential profiles of copper-induced ROS generation in human neuroblastoma and astrocytoma cells. Brain Res Mol Brain Res 134, 323–332. [PubMed: 15836927]

[50]. Chou CH, Fan HC, Hueng DY (2015) Potential of neural stem cell-based therapy for Parkinson's disease. Parkinsons Dis 2015, 571475. [PubMed: 26664823]

[51]. Flierl A, Oliveira LM, Falomir-Lockhart LJ, Mak SK, Hesley J, Soldner F, Arndt-Jovin DJ, Jaenisch R, Langston JW, Jovin TM, Schulë B (2014) Higher vulnerability and stress sensitivity of neuronal precursor cells carrying an alpha-synuclein gene triplication. PLoS One 9, e112413. [PubMed: 25390032]

[52]. Dixon SJ, Lemberg KM, Lamprecht MR, Skouta R, Zaitsev EM, Gleason CE, Patel DN, Bauer AJ, Cantley AM, Yang WS, Morrison B, 3rd, Stockwell BR (2012) Ferroptosis: An iron-dependent form of nonapoptotic cell death. Cell 149, 1060–1072. [PubMed: 22632970]

[53]. Guiney SJ, Adlard PA, Bush AI, Finkelstein DI, Ayton S (2017) Ferroptosis and cell death mechanisms in Parkinson's disease. Neurochem Int 104, 34–48. [PubMed: 28082232]

[54]. Tuszynska I, Magnus M, Jonak K, Dawson W, Bujnicki JM (2015) NPDock: A web server for protein-nucleic acid docking. Nucleic Acids Res 43, W425–W430. [PubMed: 25977296]

[55]. Ulmer TS, Bax A, Cole NB, Nussbaum RL (2005) Structure and dynamics of micelle-bound human alpha-synuclein. J Biol Chem 280, 9595–9603. [PubMed: 15615727]

[56]. Brennan RG, Matthews BW (1989) The helix-turn-helix DNA binding motif. J Biol Chem 264, 1903–1906. [PubMed: 2644244]

[57]. Moriyama T, Sangel P, Yamaguchi H, Obuse C, Miyamoto Y, Oka M, Yoneda Y (2015) Identification and characterization of a nuclear localization signal of TRIM28 that overlaps with the HP1 box. Biochem Biophys Res Commun 462, 201–207. [PubMed: 25960296]

[58]. Bunch H, Calderwood SK (2015) TRIM28 as a novel transcriptional elongation factor. BMC Mol Biol 16, 14. [PubMed: 26293668]

[59]. Sangchot P, Sharma S, Chetsawang B, Porter J, Govitrapong P, Ebadi M (2002) Deferoxamine attenuates iron-induced oxidative stress and prevents mitochondrial aggregation and alpha-synuclein translocation in SK-N-SH cells in culture. Dev Neurosci 24, 143–153. [PubMed: 12401952]

[60]. Bharathi, Indi SS, Rao KS (2007) Copper- and iron-induced differential fibril formation in alpha-synuclein: TEM study. Neurosci Lett 424, 78–82. [PubMed: 17714865]

[61]. Bharathi Rao KS (2007) Thermodynamics imprinting reveals differential binding of metals to alpha-synuclein: Relevance to Parkinson's disease. Biochem Biophys Res Commun 359, 115–120. [PubMed: 17531952]

[62]. Hegde ML, Anitha S, Latha KS, Mustak MS, Stein R, Ravid R, Rao KS (2004) First evidence for helical transitions in supercoiled DNA by amyloid Beta Peptide (1–42) and aluminum: A new insight in understanding Alzheimer's disease. J Mol Neurosci 22, 19–31. [PubMed: 14742907]

[63]. Gupta VB, Monica FS, Berrocal R, Rao KS, Rao KS (2013) Studies on the mechanism of the DNA nicking property of amyloid-β40: Implications in Alzheimer's disease. J Alzheimers Dis 33, 1059–1071. [PubMed: 23160010]

[64]. Yin S, Fan X, Yu S, Li C, Sy MS (2008) Binding of recombinant but not endogenous prion protein to DNA causes DNA internalization and expression in mammalian cells. J Biol Chem 283, 25446–25454. [PubMed: 18622017]

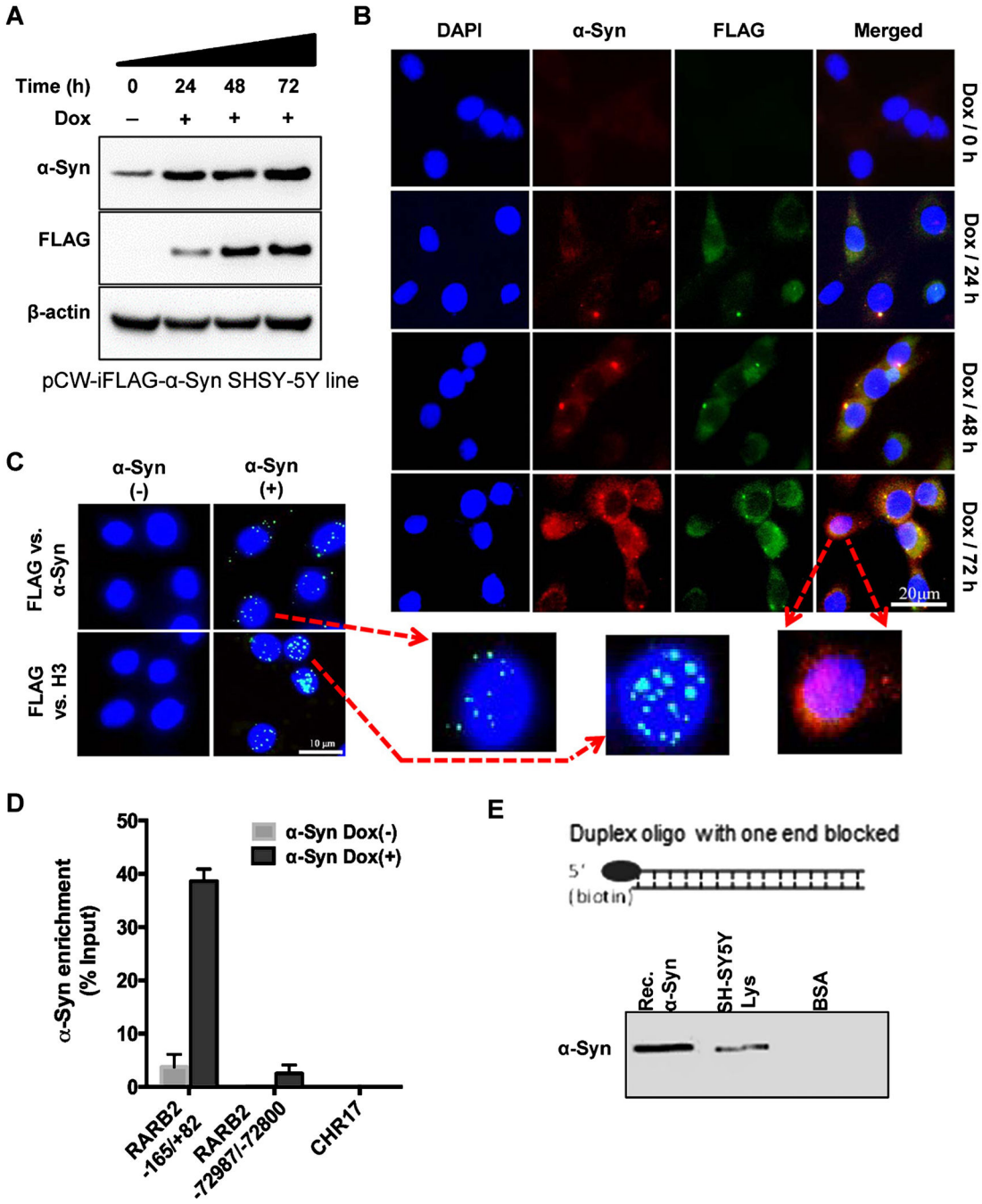

Fig. 1.

Nuclear localization and chromatin/DNA binding of α-Syn. A, B) Characterization of time-dependent induction of FLAG-α-Syn in a SHSY-5Y cell line stably harboring tet-on (Dox-inducible) pCW-iFLAG-α-Syn vector. Immunoblotting (A) and immunofluorescence (B) revealed a time-dependent increase (2–4-fold) in both FLAG and total α-Syn levels after induction with Dox for 24–72 h in differentiated cells. The presence of nuclear α-Syn after 72 h of Dox induction is indicated in the enlarged image. C) PLA of FLAG versus α-Syn antibody in pCW-iFLAG-α-Syn SHSY-5Y cells. A PLA focus in the nucleus (DAPI)

detected the same molecule of ectopic α-Syn. PLA of FLAG versus histone H3 antibody confirmed interaction with H3 in the nucleus. D) ChIP assay using FLAG antibody from pCW-iFLAG-α-Syn SHSY-5Y cells after Dox induction (72 h) and real-time PCR amplification using three randomly selected primer pairs. E) *In vitro* biotin affinity co-elution analysis. Immunoblotting of SHSY-5Y cell nuclear extract or recombinant α-Syn co-eluted with biotin-labeled duplex DNA oligo.

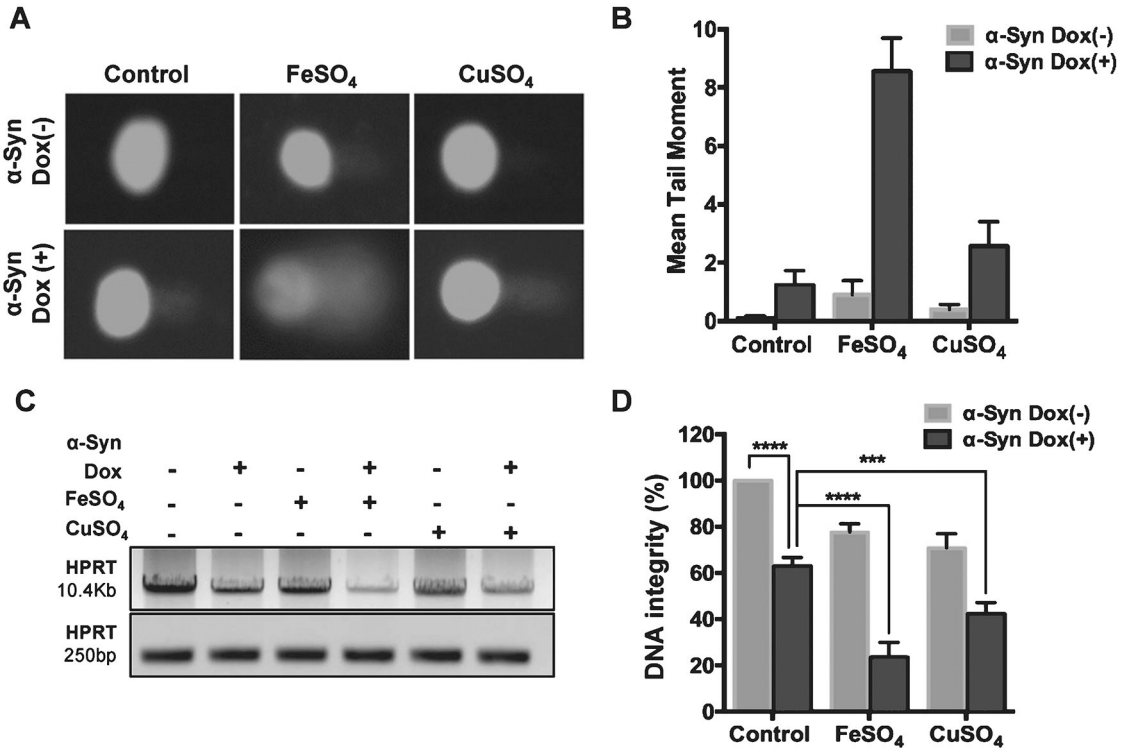

Fig. 2.

Increased α-Syn expression causes DNA breaks in neurons synergistically with pro-oxidant metals. A, B) Alkaline Comet assay in iFLAG-α-Syn SHSY-5Y cells exposed to 200 μM $FeSO_4$ or $CuSO_4$. α-Syn was induced with Dox for 48 h. Metal salts alone at the same concentration caused only moderate increases in strand breaks. C, D) Semi-quantitative LA-PCR assay for genomic DNA isolated from pCW-iFLAG-α-Syn SHSY-5Y cells in the presence of $FeSO_4$ or $CuSO_4$. ***$p \leq 0.001$; ****$p \leq 0.0001$.

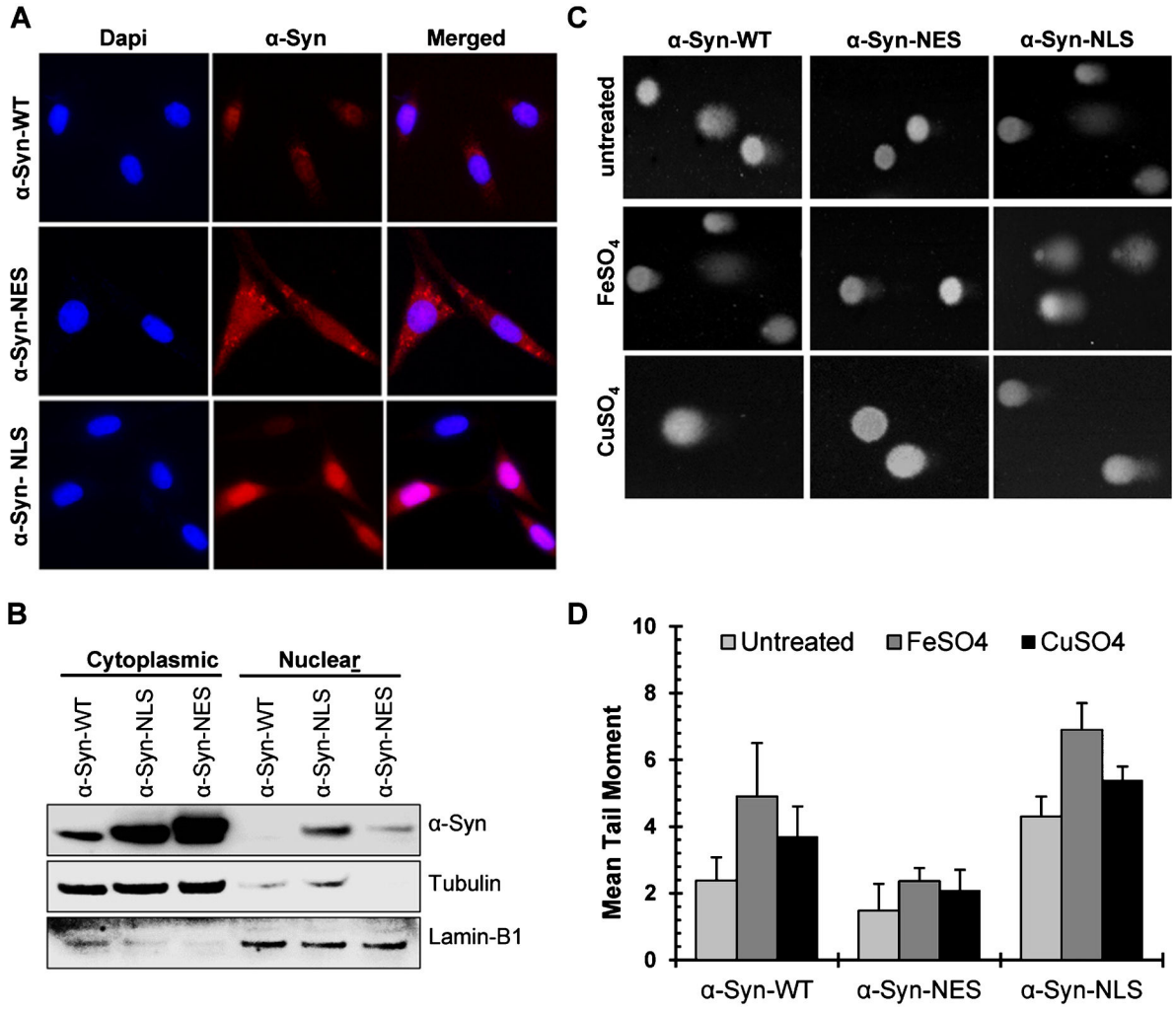

Fig. 3.

Nuclear α-Syn is required for inducing genome damage in neurons. A) Immunofluorescence images demonstrating nucleus- or cytoplasm-specific expression of mutant α-Syn vectors containing additional NES or NLS after their transient transfection in SHSY-5Y cells. B) Immunoblotting of cytosolic and nuclear fractions from WT-, NES-, and NLS-α-Syn-expressing SHSY-5Y cells. C, D) Alkaline Comet assay in NLS-, NES-, or WT-α-Syn-expressing cells with or without $FeSO_4$ or $CuSO_4$.

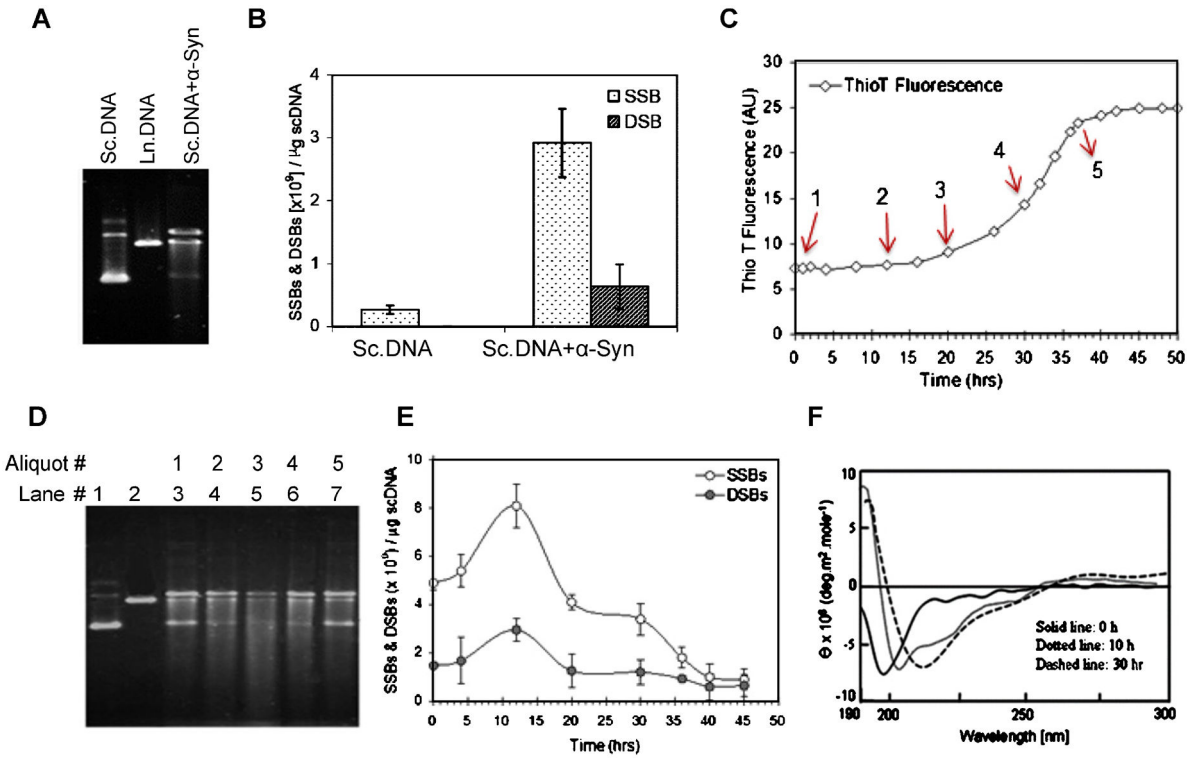

Fig. 4.

Recombinant α-Syn nicks naked DNA *in vitro*, which is enhanced by its misfolding/oligomerization. A) Agarose gel electrophoresis showing plasmid scDNA cleavage by recombinant α-Syn. B) Assessment of SSBs and DSBs in scDNA induced by α-Syn. Values are expressed as SSBs and DSBs induced per µg of scDNA. C) Recombinant α-Syn was incubated with constant stirring to cause its aggregation, which was monitored by Thio T fluorescence analysis with an aliquot of α-Syn taken at various time intervals. D) The α-Syn aliquots were also analyzed for their DNA nicking activity with plasmid DNA by agarose gel electrophoresis. E) DNA breaks were quantified. F) Misfolding/β-sheet formation in α-Syn upon stirring as confirmed by CD spectroscopy.

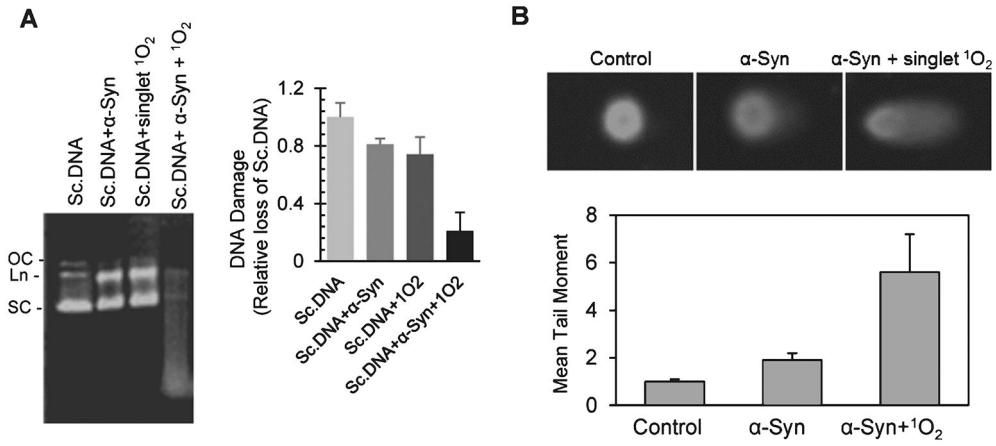

Fig. 5.

α-Syn DNA nicking activity may be mediated by its oxidation. A) Exposure of recombinant α-Syn to $^1O_2$, generated by exposing flavonoid Bengal red to UVB radiation, enhanced its DNA nicking activity with plasmid scDNA *in vitro*. The products were analyzed by agarose gel electrophoresis. The histogram represents quantification of DNA fragmentation. B) SHSY-5Y cells were exposed to similarly oxidized α-Syn, and DNA damage was quantified by alkaline Comet assay.

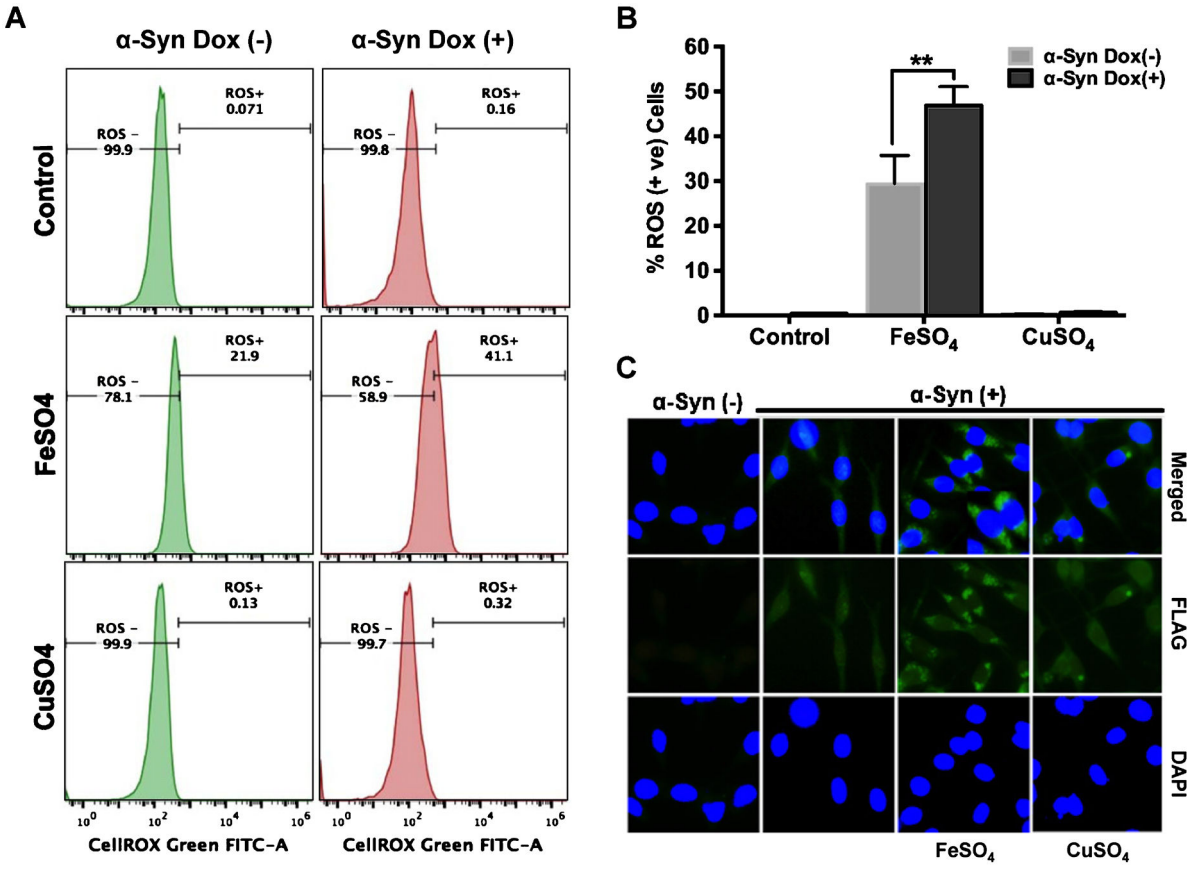

Fig. 6.

Fe-dependent ROS generation and α-Syn aggregation in pCW-iFLAG-α-Syn SHSY-5Y cells. A, B) Cells treated with $FeSO_4$ but not $CuSO_4$ showed a significant increase in nuclear and mitochondrial ROS load. Results are presented as percentage of ROS-positive cells; error bars in the histogram represent the standard error of the mean (SEM) from three independent experiments. C) Immunofluorescence indicates α-Syn aggregate formation in $FeSO_4$-treated cells. $^{**}p \leq 0.01$.

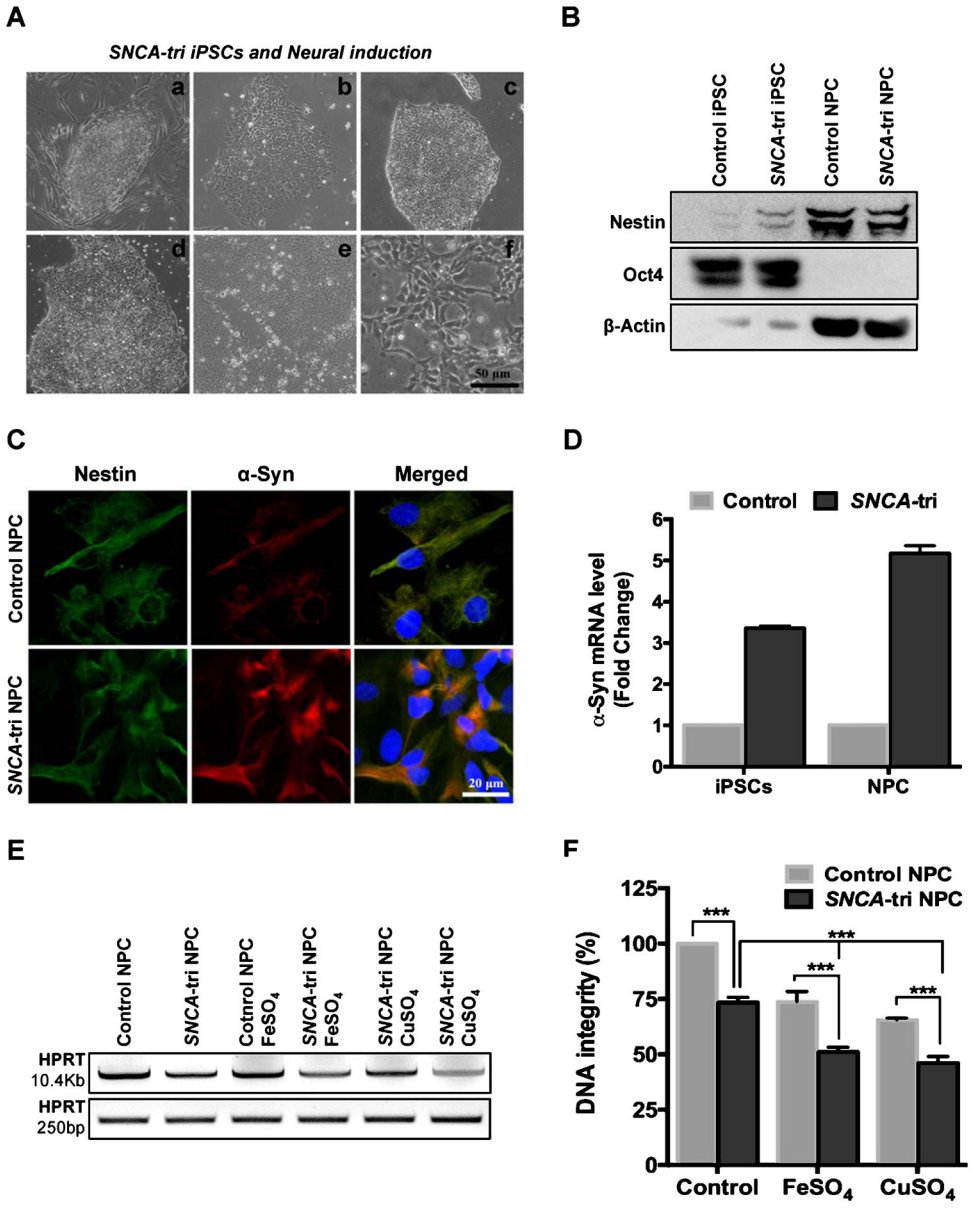

Fig. 7.

DNA damage in neurons generated from normal and PD patient-derived *SNCA*-tri iPSC cells. A) Phase contrast image demonstrating generation of NPCs from iPSCs: (a) *SNCA*-tri iPSCs cultured in MEF feeder layer, (b) *SNCA*-tri iPSCs cultured in feeder free layer, (c) day 2, (d) day 4, (e) day 6 of neural induction for NPC derivation, (f) NPC at passage 3. The iPSC specific marker Oct4 and neural precursor markers nestin analyzed by immunoblotting (B). C) Immunofluorescence characterization with nestin and α-Syn protein expression. D) α-SYN mRNA quantitation in control versus SNCA-tri iPSC and NPC cells. E, F) LA-PCR analysis of genomic DNA isolated from control or *SNCA*-tri NPC cells exposed to 200 μM $FeSO_4$ or $CuSO_4$. ***$p \leq 0.001$.

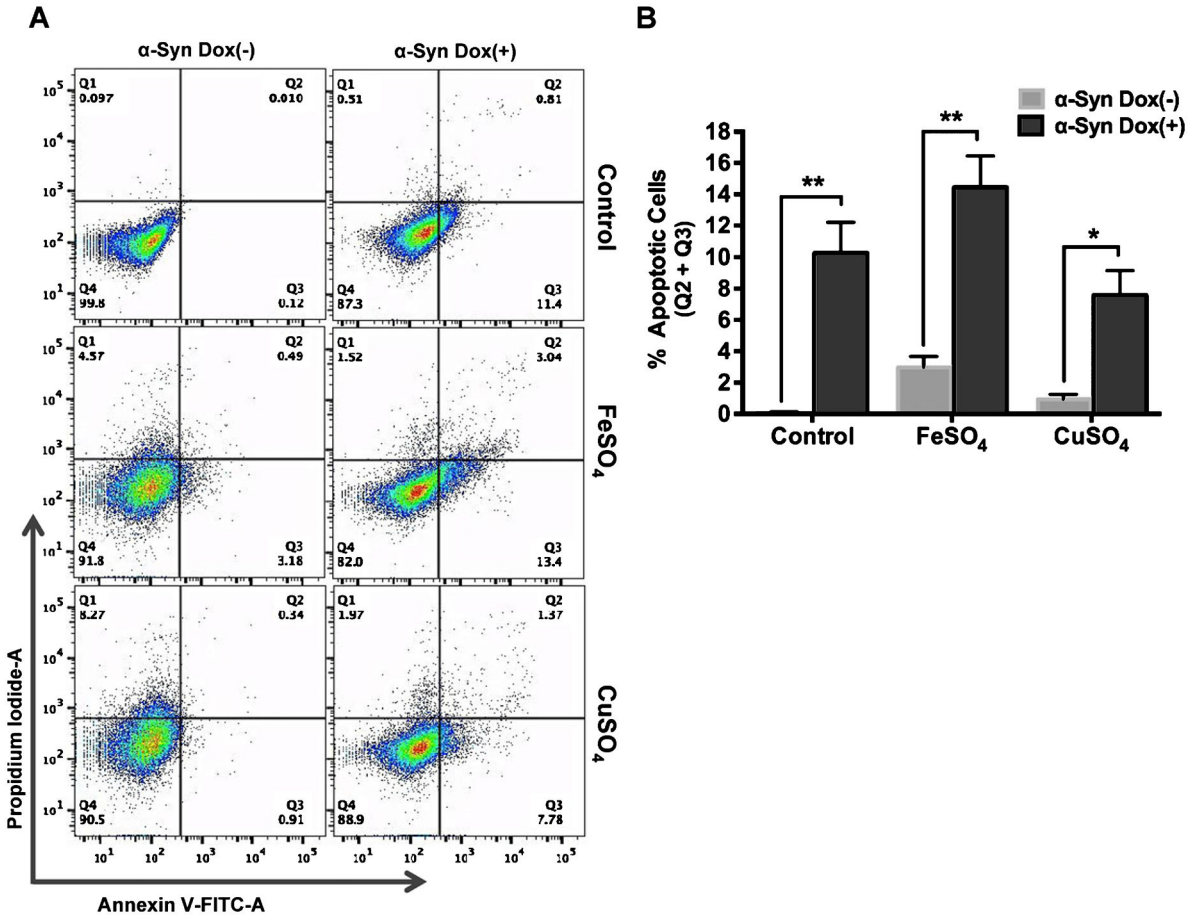

Fig. 8.

α-Syn and Fe synergistically induce neuronal apoptosis. A) pCW-iFLAG-α-Syn SHSY-5Y cells were induced with Dox for 48 h and then treated with 200 μM $FeSO_4$ or $CuSO_4$ for 24 h before being double-stained with Annexin V/PI and analyzed by flow cytometry. B)Results are presented as percentage of total apoptotic cells (early apoptotic (Q3)+ late apoptotic (Q2)). Error bars represent the SEM from three independent experiments. Fe or Cu alone caused a 4–8% necrosis (Q4) in uninduced cells, which was prevented by α-Syn induced cells. *$p \leq 0.05$; **$p \leq 0.01$.

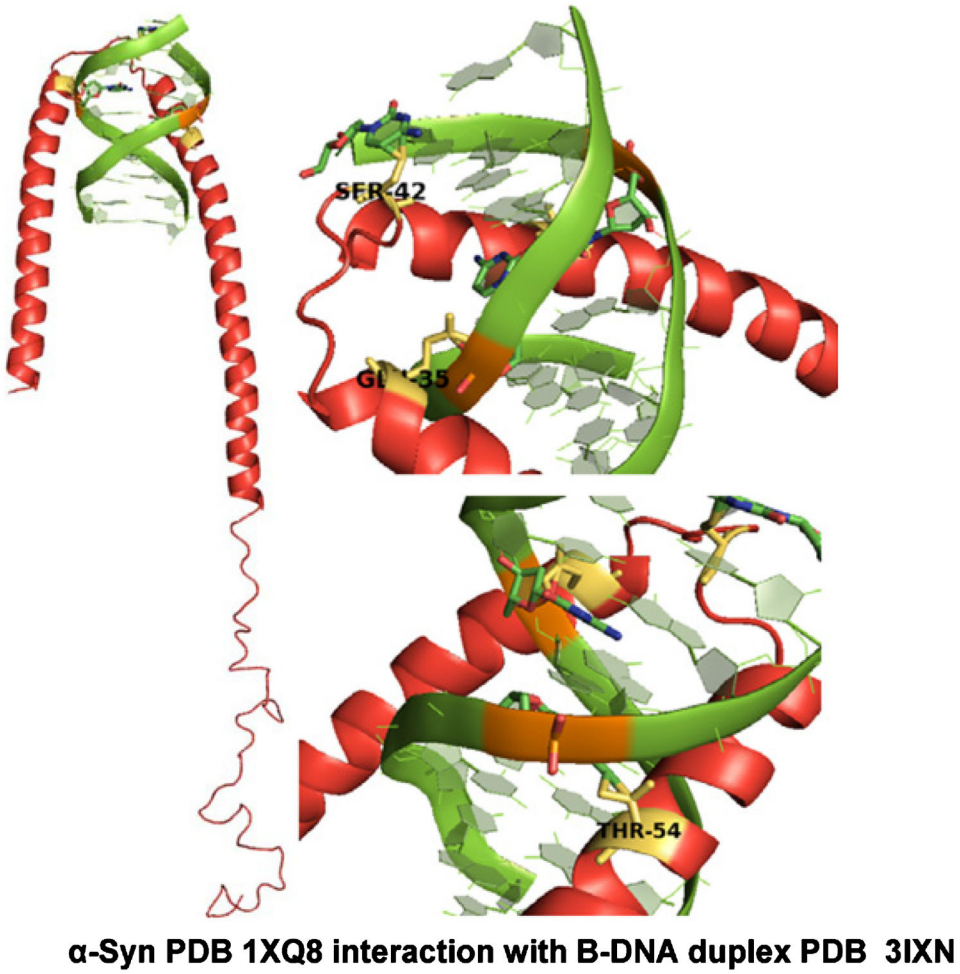

Fig. 9.

MD simulation: α-Syn N-terminal residues may be involved in DNA binding. Protein-DNA docking Model 1 demonstrating binding of α-Syn (PDB: 1XQ8) N-terminal amino acid residues Glu-35, Ser-42, Thr-54 to the crystal structure of d(CCGGTACCGG) as a B-DNA duplex (PDB: 3IXN). This structure model represents the best structure from the biggest cluster after the refinement process. Structures were analyzed using PyMOL Molecular Graphics System, Version 1.7.4.5 Schrödinger, LLC.

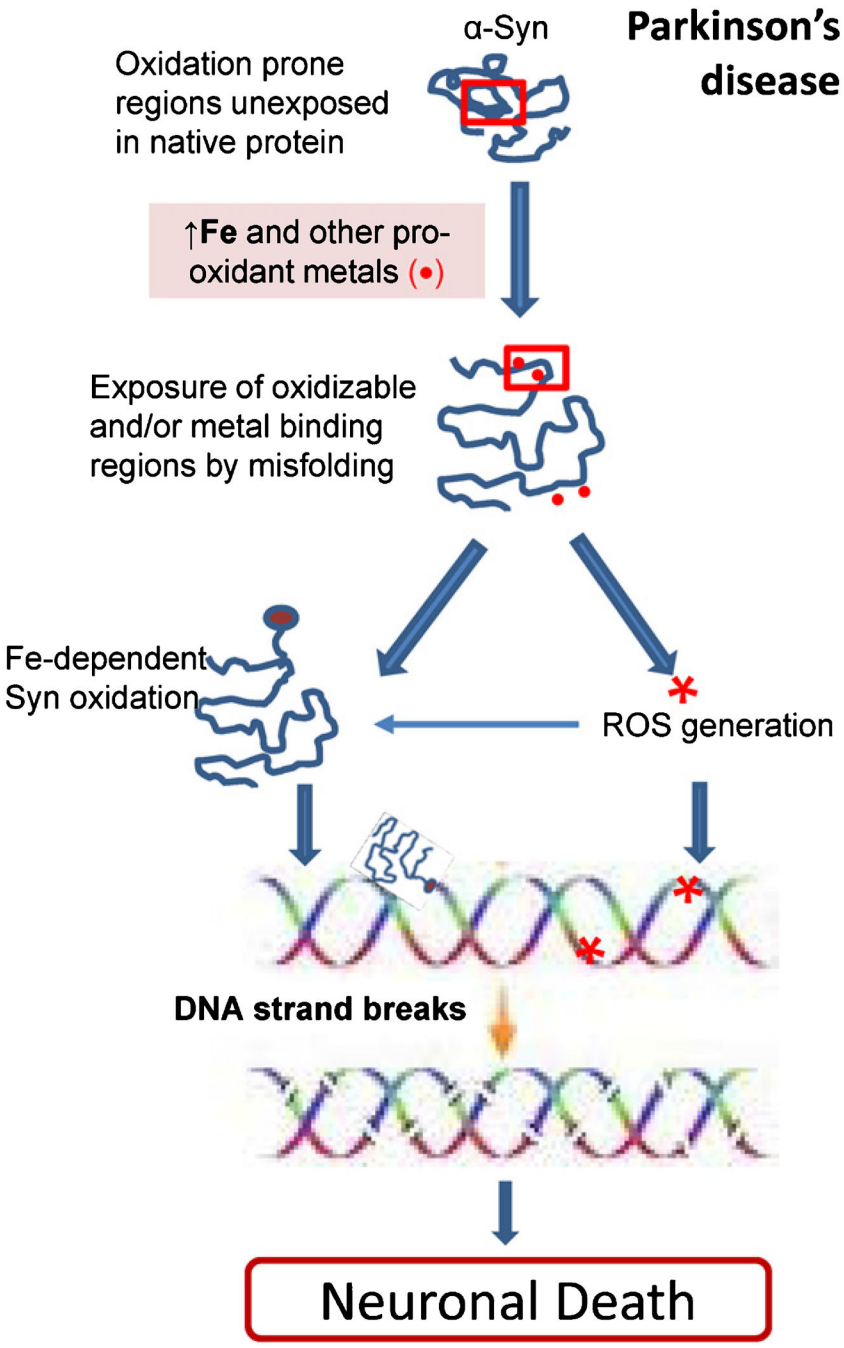

Fig. 10.

Model illustrating how α-Syn-induced DNA breaks contributes to neuronal apoptosis in PD. The role of pro-oxidant Fe or ROS in promoting α-Syn misfolding and oxidation, which could exacerbate its DNA nicking activity.